Computational approaches to asymmetric synthesis

David Balcells[ab] and Feliu Maseras*[ab]

Received (in Montpellier France) 26th October 2006, Accepted 4th January 2007
First published as an Advance Article on the web 23rd January 2007
DOI: 10.1039/b615528f

Theoretical chemistry has been successfully used as a powerful tool to obtain valuable insight into the mechanism and the origin of enantioselectivity in several asymmetric reactions of high interest. In this Perspective article, the application of QM, MM and QM/MM methods to the rationalization of electronic and steric effects upon enantioselectivity is briefly reviewed, considering some representative contributions of the last three decades.

David Balcells was born in Sant Martí de Tous (Catalonia, Spain) in 1978. In 2001, he received his Bachelor of Science degree in chemistry at the Universitat Autónoma de Barcelona. From 2001 to 2006, he worked on a PhD project under the guidance of Dr Feliu Maseras, firstly at the Universitat Autónoma de Barcelona (2001–2003) and afterwards at the Institute of Chemical Research of Catalonia (2004–2006). David's research focused on applications of computational chemistry to the study of the asymmetric synthesis of chiral sulfoxides. In 2006, he obtained his PhD degree in chemistry. Very recently, he obtained a postdoctoral fellowship to work at the Université Montpellier 2 with Odile Eisenstein.

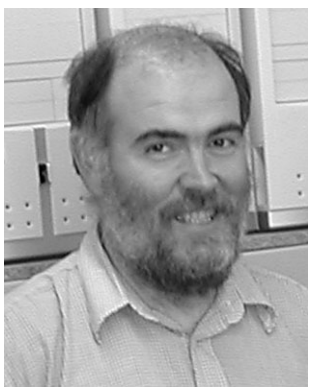

Feliu Maseras was born in 1962 in Martorelles, Catalonia. He studied at the Universitat Autónoma de Barcelona, where he obtained his BSc in 1985 and his PhD in 1991. He then spent two years as a postdoctoral fellow with Keiji Morokuma at the Institute for Molecular Science in Okazaki, Japan. After a two year position as a CNRS Associate Researcher in the group of Odile Eisenstein in Montpellier, France, he took the position of Associate Professor at the Universitat Autónoma de Barcelona in 1998. He moved to his current position as Research Group Leader at the Institute of Chemical Research of Catalonia in 2004. His current research interests involve the development and application of theoretical methods to transition metal compounds, with special focus on the use of hybrid methods combining quantum mechanics and molecular mechanics for modelling species of experimental interest.

1. Introduction

The progress of computational chemistry in recent years is undeniable, and can be easily measured by the number of scientific publications and their impact on experimental research. The most immediate cause of this recent development has been the ever increasing capability of computer hardware, with the accompanying implementation of new theoretical software. However, the key to computational chemistry is not the power of the computer, but the skill of the computational chemist. It is, in this sense, instructive to see how several decades ago, when computers were much more rudimentary, useful insight into practical problems could already be gained from theoretical studies. These early works laid the ground, on which modern applied computational chemistry is based. One of these pioneering articles was published in the first volume of *Nouveau Journal de Chimie* by Nguyen Trong Anh and Eisenstein,[1] dealing with the difficult topic of asymmetric synthesis. The success of the work can be measured by the more than 500 citations it has already collected. This Perspective will give some examples of how computational research on the topic has progressed in the last three decades.

The synthesis of chiral compounds is a prominent field of research in modern chemistry. Chiral compounds have a broad range of applications as drugs,[2–5] polymers,[6–9] probes of biological function[10–13] and new materials.[14–17] In fact, a whole new industry focused on chirality exists nowadays.[18] In general, the optimal properties of chiral compounds are only achieved when they are prepared in a pure single enantiomer form. Moreover, in exceptional cases, one of the enantiomers can be toxic.[19] The growing public awareness of health issues is prompting the application of new laws concerning the optical purity of drugs around the world.[20,21] These laws force the pharmaceutical industry to prepare and commercialize their products as single enantiomers.

[a] *Institute of Chemical Research of Catalonia (ICIQ), Avgda. Països Catalans 16, 43007 Tarragona, Catalonia, Spain*
[b] *Unitat de Química Física, Edifici Cn, Universitat Autónoma de Barcelona, 08193 Bellaterra, Catalonia, Spain. E-mail: fmaseras@iciq.es*

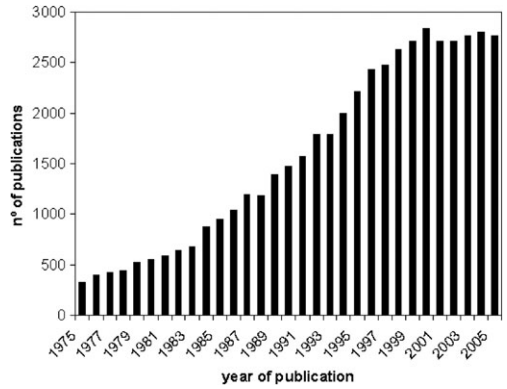

Fig. 1 Number of publications containing the keywords "optically active", "chiral" or "asymmetric synthesis" in their title *vs.* year of publication. Data extracted from the ISI Web of Knowledge.™

Optically active compounds are prepared, in most cases, by means of asymmetric synthesis. This approach consists of transforming non-chiral substrates by generating new stereogenic centers of particular configuration. The importance of optically active chiral compounds and asymmetric synthesis can be easily understood by inspecting Fig. 1. In this Figure, the number of publications containing the keywords "optically active", "chiral" or "asymmetric synthesis" in their title is plotted against the year in which they were published. The number of publications grew exponentially from 1975 to 2000 and remained almost constant from 2000 to 2005, with more than 2700 publications each year.

The good performance of asymmetric synthesis is not a trivial issue if we keep in mind that enantiomers have the same energy. In all asymmetric transformations, chirality is generated at some point, and then the reaction diverges into two pathways, one leading to the *R* product and the other to the *S* product. If these pathways are strictly enantiomeric then they are isoenergetic, and the product of the reaction is a racemate (see Fig. 2). This problem is solved by using the same property that is desired in the reaction product: chirality. Chiral compounds with a well defined and stable configuration are used to obtain non-degenerate diastereomeric pathways, leading to the target product in an enantioselective fashion. Hence, chiral compounds are also crucial as a tool to obtain other optically active products. Formally, the most simple enantioselective process will have a chiral compound as a substrate. To achieve chirality from non-chiral substrates, chiral compounds are used in asymmetric synthesis in three different manners: (1) as chiral auxiliaries, like menthol,[22,23] (2) as chiral reagents, like optically active oxaziridines[24] and peroxides,[25] and (3) as chiral catalysts (asymmetric catalysis[26]). The latter approach is the most convenient, since it does not require stoichiometric amounts of chiral compounds, which are usually expensive or not easily accessible. In 2001 Nobel Prize for chemistry was given to Knowles,[27] Sharpless[28] and Noyori[29] "for their work on chirally catalyzed hydrogenation and oxidation reactions".

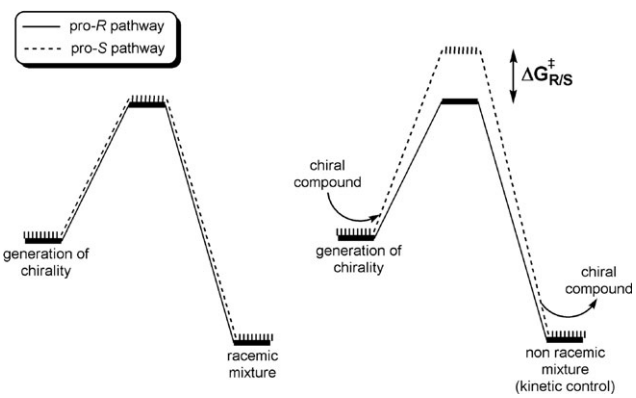

Fig. 2 Enantiomeric (left) and diastereomeric (right) reaction pathways in asymmetric synthesis.

The basic concept for the computational calculation of enantioselectivity is quite simple. In asymmetric synthesis, enantioselectivity has been traditionally quantified by evaluating the enantiomeric excess (% ee, eqn. (1)). We will briefly discuss here how it can be obtained from computational data. Similar reasonings could also be applied to obtain other parameters, like the enantiomeric ratio.[30] Since enantioselective reactions are, in most cases, under kinetic control, ee can be computed by assuming that the final *S*/*R* ratio is given, at a certain temperature, by the Boltzmann distribution of the transition states leading to each enantiomer (eqn. (2)). Combining eqn. (1) and eqn. (2), we can easily compute ee (eqn. (3)) from the free energy difference between the pro-*R* and pro-*S* transition states ($\Delta G^{\ddagger}_{R/S}$ in Fig. 2). The tools provided by modern computational chemistry[31] can be used to estimate $\Delta G^{\ddagger}_{R/S}$, and this can be useful, not only to predict enantioselectivity, but also to rationalize it, predict tendencies and tackle the optimization of a given method of asymmetric synthesis in a rational fashion.

$$\%\ \mathrm{ee} = \frac{[R]-[S]}{[R]+[S]} \times 100 \qquad (1)$$

$$\frac{[S]}{[R]} = \mathrm{e}^{-\Delta G^{\ddagger}_{R/S}/RT} \qquad (2)$$

$$\%\ \mathrm{ee} = \frac{1-\mathrm{e}^{-\Delta G^{\ddagger}_{R/S}/RT}}{1+\mathrm{e}^{-\Delta G^{\ddagger}_{R/S}/RT}} \times 100 \qquad (3)$$

The methods based on quantum mechanics[32] (QM methods) provide the most accurate description, and can be used to model bond formation and cleavage, and thus reactivity. QM methods like density functional theory[33] (DFT) have been used as powerful tools in the elucidation of reaction mechanisms.[34,35] These methods have been successfully used to clarify the mechanism of several metal-catalyzed reactions used in organic synthesis, like σ-bond activation,[36] the hydrogenation of carbon dioxide,[37] terscSaka79 olefin polymerization,[38] the isomerization of double and triple carbon–carbon bonds,[39] oxygen transfer reactions,[40] benzannulation[41] and coupling reactions (Heck,[42] Suzuki[43] and Stille[44] reactions). QM methods can be also used to predict and rationalize enantioselectivity when electronic effects play a key role. One of the first and most appealing applications of QM methods to the rationalization of stereochemistry was the theoretical study

on 1,2-asymmetric induction published by Nguyen Trong Anh and Eisenstein in *Nouveau Journal de Chimie* 30 years ago.[1]

The main drawback of QM methods is that they are very time-consuming, especially when the system under study is big. This problem is overcome using the methods based on molecular mechanics (MM methods). These methods are fast and able to provide a good description of the steric effects that, in most cases, control the enantioselectivity of asymmetric catalysis.[45,46] Nevertheless, their application to the study of reactivity, although possible,[47,48] is seriously complicated by the intrinsic difficulty MM methods have in describing processes that involve the forming or breaking of chemical bonds.

When the system is large and we need to introduce both electronic effects, to model reactivity, and steric effects, to rationalize enantioselectivity, the best deal is often offered by hybrid QM/MM methods, which offer a good description of the system in a reasonable time.[49] These methods are applied by dividing the system into two parts, one computed at the QM level (QM part) and the other at the MM level (MM part). QM/MM methods have been widely used in the study of asymmetric catalysis. In these studies, the QM part typically includes the metal and its close surroundings, where the reaction takes place, while most of the bulky chiral ligand is embedded within the MM part. Furthermore, the reaction mechanism is usually disclosed in a preliminary QM study on the model system, and the origin of the enantioselectivity is subsequently determined at a QM/MM level.[50] This strategy has been successfully applied to the study of several catalytic systems used in asymmetric hydrogenation,[51,52] hydroformylation,[53,54] hydrosilylation,[55] sulfoxidation[56,57] and olefin dihydroxylation.[58,59] Tacticity control in olefin polymerization is also a stereochemical issue that has been intensely studied from a computational point of view.[60–63]

In this Perspective article, a brief review of computational research in the area of asymmetric synthesis is made, based on a summary of work that has been published over the years. This is not a systematic review, but an attempt to show, through selected examples, how different tools have been applied to deal with different practical issues, with an emphasis on recent QM/MM applications. Among worthy contributions that are not discussed here, one can mention calculations using semi-empirical methods,[64] and applications of recently developed methods with problem-tailored force fields[65] and quantitative structure selectivity relationships.[66]

2. QM studies. Electronic effects

2.1 (1,2)-Asymmetric induction in the nucleophilic addition to chiral carbonyl compounds

1,2-Asymmetric induction in nucleophilic addition to chiral carbonyl compounds[67,68] is a paradigm of organic stereochemistry. The two possible diastereofacial approaches of nucleophile Nu^- to the carbonyl plane lead to different diastereomeric products (see Fig. 3). The stereochemical outcome of this reaction had been traditionally rationalized by means of the Cram,[69] Cornforth,[70] Karabatsos[71] and Felkin[72,73] models. In all of these models, the small, medium and large substituents of the chiral carbon (C*) attached to the

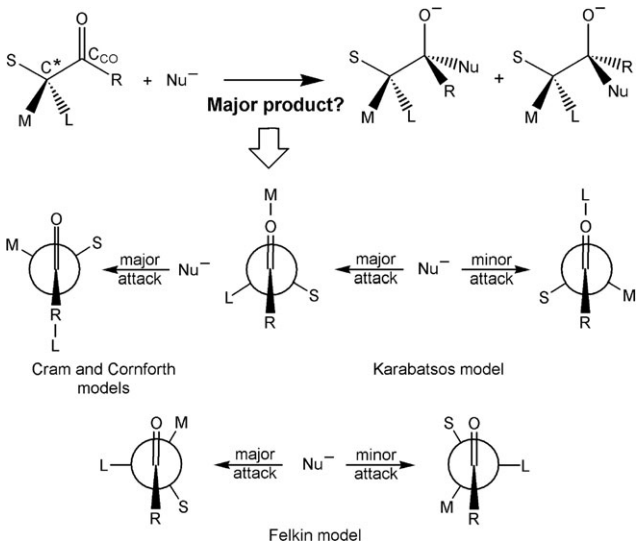

Fig. 3 Traditional models to rationalize 1,2-asymmetric induction in nucleophilic addition to chiral carbonyl compounds.

carbonyl carbon (C_{CO}) are labelled as S, M and L, respectively. Furthermore, a perpendicular approach of the nucleophile to the carbonyl plane is assumed. In the Cram, Cornforth and Karabatsos models, the reactant approaches the face of the carbonyl plane occupied by the smaller substituent. In the Felkin model, the nucleophilic reagent bisects the C*–S and C*–M bonds. These simple models are used by organic chemists in order to predict the absolute configuration of the major reaction product.

The validity of these qualitative models was theoretically assessed by Nguyen Trong Anh and Eisenstein.[1] This work was one of the first examples of how QM methods can be successfully used to understand the stereochemical outcomes of organic reactions.[74] The nucleophilic addition of H^- to (Me)(Cl)CH–CHO and (Me)(Et)CH–CHO was studied through an *ab initio* STO-3G study. Twenty four conformations of the transition state, corresponding to the twelve rotamers of the molecule and the two diastereofacial approaches of the nucleophile, were considered. The theoretical study on the addition of H^- to (Me)(Cl)CH–CHO revealed that the most stable transition states corresponded to the Felkin model. The authors demonstrated that the coulombic repulsions between the hydride anion and the chlorine atom did not play a relevant role, since the same conclusion was reached in the case of (Me)(Et)CH–CHO.

The effect of the counter-cation and the influence of the solvent (water) were explored by introducing $CO\cdots Li^+$ and $H^-\cdots HOH$ interactions into the system. The results showed that the Felkin model was essentially not affected by these factors, since no major structural modification of the preferred transition states was found. The stereoelectronic influence upon the direction of the nucleophile approach, related to the $O–C_{CO}–H^-$ angle of attack (α), was also analyzed, and the results showed that the orientation was not completely perpendicular ($98^\circ < \alpha < 109^\circ$). This result suggested that the discrimination between the two Felkin transition states was not only given by the steric interactions between O and M, but also by those between the nucleophile and M.

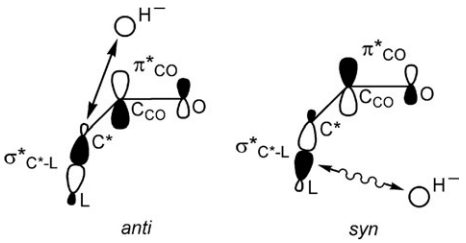

Fig. 4 Molecular orbital interactions in *anti* and *syn* nucleophilic additions.

Nguyen Trong Anh and Eisenstein proved that the suitability of the Felkin model was due to the antiperiplanar orientation of the nascent H^{-}–C_{CO} bond with respect to the C*–L bond. The antiperiplanar effect was found to be more relevant than the orbital distortion influence on the direction of reagent approach. The preference for the antiperiplanar arrangement was rationalized in terms of frontier molecular orbital interactions between the HOMO of H^{-} and the LUMO of the electrophilic carbonyl compound, composed of antibonding $\sigma^{*}_{C^{*}-L}$ and π^{*}_{CO} orbitals (see Fig. 4). Whereas the *anti* approach of H^{-} is characterized by bonding interactions with $\sigma^{*}_{C^{*}-L}$, the *syn* approach involves antibonding interactions. This MO scheme allows determination of the effective size of substituents attached to C* (R = S, M and L) by inspecting the energies of the antibonding $\sigma^{*}_{C^{*}-R}$ orbitals.

2.2 Proline-catalyzed asymmetric aldol and related reactions

Asymmetric organocatalysis is an emerging powerful tool for the synthesis of chiral compounds.[75–78] This synthetic approach avoids one of the main concerns in industry: the elimination of metal-related impurities in the final product.[79] The proline-catalyzed intramolecular aldol cyclization of triketones was one of the first examples of asymmetric organocatalysis (see Fig. 5). This reaction was independently developed by the groups of Hajos[80] and Wiechert,[81] and successfully applied to obtain useful structural building blocks for the total synthesis of natural products.[82–85]

Two different reaction mechanisms were proposed by Hajos and Parrish:[80] (1) a nucleophilic substitution mechanism involving a carbinolamine intermediate, in which proline is initially added to a carbonyl of the cyclic ketone, and (2) an enaminium-catalyzed mechanism involving an enamine intermediate, which implies the initial condensation of proline with the side chain ketone. The latter reaction pathway (mechanism **I** in Fig. 6) was supported by experimental studies,[86–88] showing the participation of enamine intermediates.

Proline-catalyzed asymmetric aldol and related reactions have been theoretically studied by the group of Houk.[89]

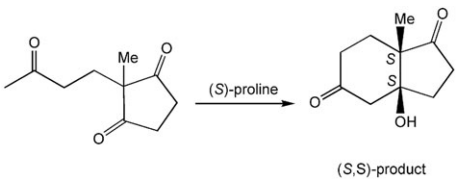

Fig. 5 Proline-catalyzed aldol reaction.

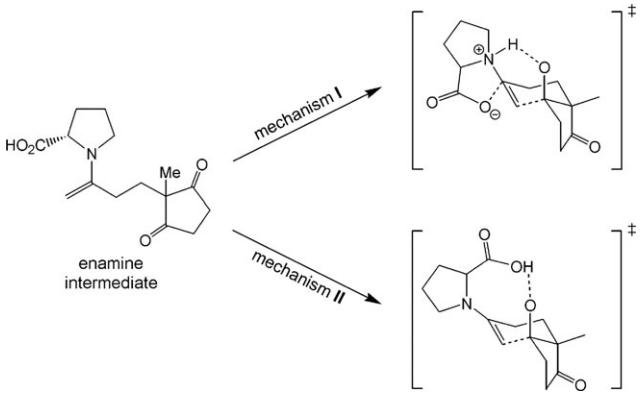

Fig. 6 Proposed mechanisms for the proline-catalyzed aldol reaction.

A DFT(B3LYP)[90,91] 6-31g(d) study on the reaction represented in Fig. 5 revealed that the lowest energy reaction pathway implied the participation of an enamine intermediate.[92,93] This study also supported the hypothesis that the formation of the C–C bond is coupled with a hydrogen transfer to the developing alkoxide. In the enamine mechanism originally proposed by Hajos and Parrish,[80] such hydrogen transfer involved the NH group of proline (mechanism **I** in Fig. 6). In contrast to this, Houk demonstrated that the group participating in hydrogen transfer is the COOH (mechanism **II** in Fig. 6). Furthermore, the participation of an additional molecule of proline, assisting the hydrogen transfer, was discarded in a combined experimental/theoretical study by Houk *et al.*[94]

The computational studies reported by Houk not only clarified the reaction mechanism but also provided a powerful steric model capable of rationalizing and predicting the origin of the enantioselectivity.[95] The two diastereomers of the transition state are distinguished by the conformation of the C–N bond. While, in the pro-(*S*,*S*) saddle point, the carboxylic group is *anti* to the enamine double bond, in the pro-(*R*,*R*), it is *syn* (see Fig. 7). The calculations predicted that the *anti*-(*S*,*S*) transition state is more stable than the *syn*-(*R*,*R*) by 3.4 kcal mol^{-1}, in total agreement with the experiments.[80,81] The higher stability of the *anti*-(*S*,*S*) saddle point was due to three different factors: (1) an optimal hydrogen transfer arrangement, (2) the iminium double bond planarity and (3) attractive CHO interactions. This steric model was successfully applied to test, *in silico*, the performance of proline as an organocatalyst in the aldol reactions of cyclohexanone with benzaldehyde and isobutyraldehyde.[96]

The group of Houk extended their DFT studies to other relevant asymmetric organocatalytic processes including: (1) proline-catalyzed Mannich[97] and α-aminoxylation[98] reactions,

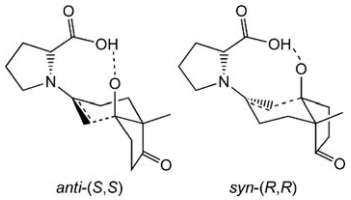

Fig. 7 Transition states for the proline-catalyzed aldol reaction.

(2) aldol reactions catalyzed by other amino acids, such as phenylalanine,[93] and (3) C–C bond-forming reactions using imidazolidinones as organocatalysts.[99,100]

3. MM and QM/MM studies. Steric effects

3.1 Stereocartography in the Diels–Alder cycloaddition

All asymmetric catalysts able to afford high enantioselectivities should have a region of chirality, or maximum stereodiscrimination, close to the site of chemistry, where the new stereogenic center of the reaction product is created (see Fig. 8). This intuitive but loosely defined hypothesis is often used by experimental chemists to tackle the design and improvement of chiral catalysts. This hypothesis was recently demonstrated and refined by Lipkowitz through the introduction of a new concept: stereocartography.[46]

Stereocartography is the mapping of the regions of maximum stereodiscrimination around a chiral catalyst. The chiral catalyst is embedded within a three-dimensional grid, in which the substrate is introduced as a probe. The intermolecular interactions between the catalyst and the probe are computed, placing the substrate at each and every grid point. Such interactions are evaluated at a MM level with the AMBER force field.[101] The possible conformations of the substrate and the catalyst are sampled, together with the different orientations of the probe, with respect to the catalyst. These calculations are performed for both the *R* and *S* probes, and the difference between the interaction energies at each grid point for both probes is then computed. The regions of maximum stereodiscrimination correspond to the isodensity contour plots encapsulating the grid points with the largest energy differences. The distance between the centroids of such plots and the site of chemistry is then computed to assess the spatial congruence between those regions.

Lipkowitz applied the concept of stereocartography to the asymmetric Lewis acid-catalyzed Diels–Alder reaction.[46] This reaction is a powerful synthetic tool[102–105] due to its ability to afford up to four stereogenic centers in a single step. The Diels–Alder cycloadditions of cyclopentadiene with three different dienophiles, including 3-((*E*)-butenoyl)-1,3-oxazolidin-2-one, acrolein and methylacrylate (see Fig. 9), were analyzed.

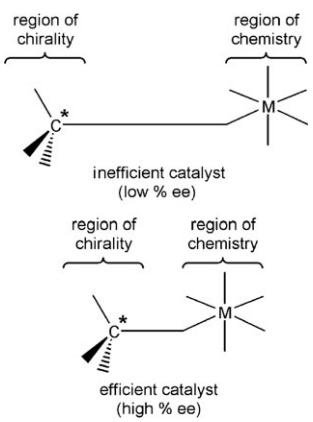

Fig. 8 Spatial congruence between the region of chirality and the site of chemistry in asymmetric catalysis.

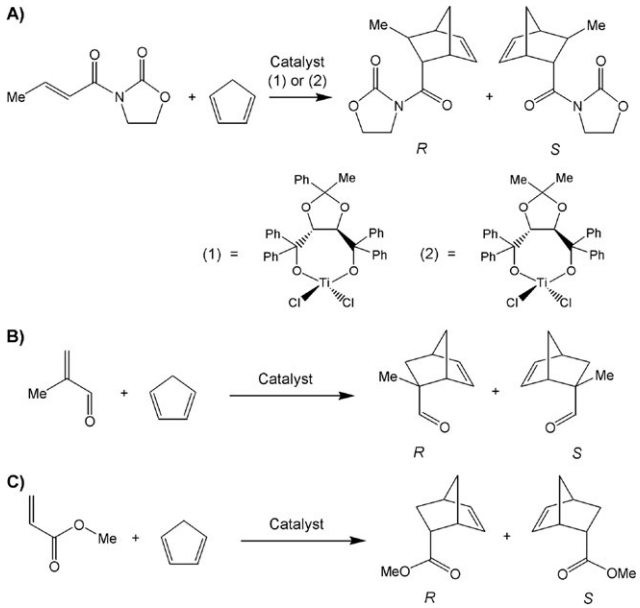

Fig. 9 Lewis acid-catalyzed asymmetric Diels–Alder reactions.

Eighteen different catalysts were considered (11 for reaction A, 5 for reaction B and 2 for reaction C), each one having a different chiral ligand and including a wide variety of metals (Mg, B, Al, Ti, Ni, Pt, Cu, Zn, Fe and Ru). Stereocartography was also later applied to the study of other catalytic systems.[106,107]

For each reaction in Fig. 9, both efficient and inefficient catalysts were considered. For 17 of the 18 systems, stereocartography calculations showed that the catalysts inducing the highest enantioselectivities were those that had the region of chemistry located close to the region of chirality, proving the reliability of the intuitive hypothesis mentioned above. One of the most interesting examples explored by Lipkowitz was the different performances of similar catalysts (1) and (2) in reaction **A** (see Fig. 9). Narasaka *et al*. found that enantioselectivity was strongly dependent on the nature of the substituents of the acetal ring.[108] This effect is quite puzzling if we consider the far-away location of these substituents with respect with the metal (site of chemistry). Whereas catalyst (1) gave 92% ee, with catalyst (2), only 55% ee was achieved. These results were rationalized by stereocartography calculations. The results revealed that the distance between the site of chemistry and the region of maximum stereoinduction increases from 1.57 Å in (1) to 5.33 Å in (2). The greater separation between these two regions of the catalyst gives rise to the ee decrease experimentally observed.

This study showed that the new computational tool developed by Lipkowitz could be used to test chiral catalysts *in silico*. Furthermore, the maps given by this technique can be used to locate and measure the regions of maximum stereodiscrimination, and this information can be applied to the rational design of new and more efficient chiral catalysts.

3.2 Asymmetric dihydroxylation of olefins

The asymmetric dihydroxylation of olefins is a powerful synthetic tool, yielding optically active 1,2-diols that can be

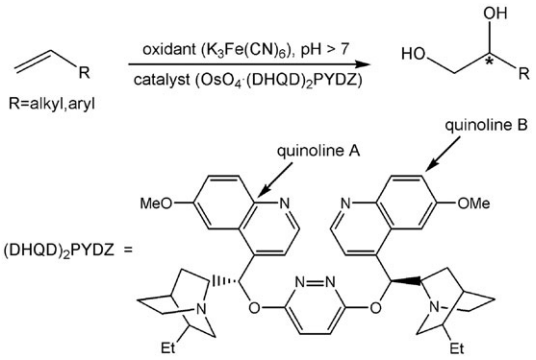

Fig. 10 Osmium-catalyzed asymmetric dihydroxylation of olefins.

subsequently used to obtain natural products.[109] The most relevant example of this synthetic approach is the osmium-catalyzed asymmetric dihydroxylation developed by the group of Sharpless,[110,111] which was awarded the Nobel Prize in chemistry in 2001.[28]

The computational study undertaken of the dihydroxylation process is a good example of how initial QM calculations on a model system can be complemented afterwards by QM/MM calculations on the real system. The mechanism of the reaction was originally a subject of controversy. Two different mechanisms were proposed: (1) the [2 + 2] stepwise mechanism, with an osmaoxetane intermediate,[112–114] and (2) the [3 + 2] concerted mechanism,[115,116] which nowadays, in a good part thanks to computational studies on model systems,[58] is generally accepted as the one that operates.[117]

The osmium-catalyzed asymmetric dihydroxylation of olefins was explored by some of our group in a series of QM/MM studies[59,118] using the IMOMM method (IMOMM stands for "Integrated Molecular Orbital Molecular Mechanics").[119] The origin of the enantioselectivity was explored in the dihydroxylation of aromatic and *n*-aliphatic olefins catalyzed by $OsO_4 \cdot (DHQD)_2PYDZ$ (see Fig. 10). In the QM part, the catalyst was modelled at the DFT(B3LYP) level as $OsO_4 \cdot NH_3$. The alkenes were modelled as either $CH_2{=}CH_2$ (aromatic olefins[59]) or $CH_2{=}CH{-}CH_3$ (*n*-aliphatic olefins[118]). The rest of the catalyst and the olefin were described with the MM3 force field. A preliminary study on the $OsO_4 \cdot NH_3$ + $CH_2{=}CH_2$ model system[58] at the DFT(B3LYP) level[90,91] revealed that this catalytic system follows the [3 + 2] concerted mechanism.

The stereochemical outcome of the reaction is controlled by the orientation in which the olefin approaches the $OsO_4 \cdot (DHQD)_2PYDZ$. This species has a distorted trigonal bipyramidal geometry, with a chiral nitrogen of the $(DHQD)_2PYDZ$ ligand and one oxygen in the axial positions. The olefin undergoes the dihydroxylation transformation, binding with the axial oxygen and one of the equatorial oxygens. These stereoelectronic requirements of the reaction imply that there are three possible regions (**A**, **B** and **C**) in which the olefin can attack the catalyst (see Fig. 11). Moreover, depending on the position of the alkene substituent, each region has four possible orientations (**I**, **II**, **III** and **IV**). Hence, a total number of twelve reaction pathways are possible.

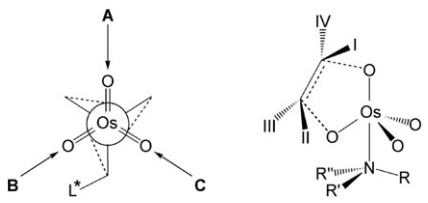

Fig. 11 Different regions (left) and orientations (right) in the olefin attack at $OsO_4 \cdot (DHQD)_2PYDZ$.

The transition states corresponding to the twelve dihydroxylation pathways were computed in the particular case of styrene.[59] The preferred region of attack is **B** since the lowest energy pro-*R* and pro-*S* transition states were **B–I** and **B–IV**, respectively. The energy difference of 2.6 kcal mol^{-1} between these saddle points indicated that the *R*-enantiomer should be formed as the major reaction product, with an ee of 99.9%, in good agreement with the experimental results[116,120] (96% ee of the *R*-product). The partition and analysis of the QM/MM energy showed that the origin of enantioselectivity is mostly due to attractive π–π face-to-face interactions between the phenyl ring of styrene and the quinoline **A** moiety of the $(DHQD)_2PYDZ$ ligand (see Fig. 10).

The QM/MM study was subsequently broadened to explore the dihydroxylation of *n*-alkenes.[118] The most relevant, but also puzzling, feature of this reaction is the dependence of enantioselectivity on the value of *n*.[121] A series of experiments showed that enantioselectivity increases sharply from 1-propene to 1-hexene, and then remains constant from 1-hexene to 1-decene (see Fig. 12). The origin of this effect was unknown and could not be rationalized in terms of π–π interactions found in the case of styrene.[59]

The dihydroxylation of *n*-alkenes is characterized by a high degree of conformational complexity, given by the flexible aliphatic chain of the olefin. This problem was solved by applying a systematic search approach, in which all the possible conformations were optimized at the MM3 level, keeping the QM part frozen.[118] The most stable geometries found at the MM level were selected and re-optimized at the more time-consuming and accurate IMOMM level. Studying the full set of *n*-alkenes, from 1-propene to 1-decene, prompted consideration of almost 40 000 conformations. A total of around 1700 transition states were selected and re-optimized at the QM/MM level. Remarkably, the results reproduced

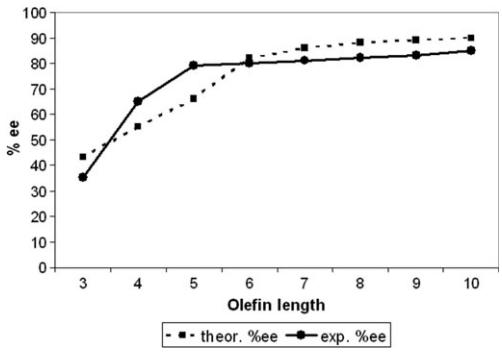

Fig. 12 Influence of the olefin chain length on enantioselectivity in the osmium-catalyzed asymmetric dihydroxylation of terminal aliphatic *n*-alkenes.

faithfully the experimental trend (see Fig. 12). As the length of the aliphatic chain increased from $n = 3$ to $n = 6$, enantioselectivity increased, and then remained almost constant within the $n = 6$ to $n = 10$ range. Analysis of the lowest-energy transition states showed that the origin of the enantioselectivity was given by attractive CH–π and hydrophobic interactions between the aliphatic chain of the olefin and the quinoline **A** and **B** rings of $(DHQD)_2PYDZ$. As the chain grows from $n = 3$ to $n = 6$, these interactions increase in number and enantioselectivity thus rises. From $n = 6$ to $n = 10$, the chain steps out of the catalyst pocket and enantioselectivity remains constant, since no more attractive interactions are established between the alkene and the ligand.

3.3 Catalytic asymmetric hydrogenation of alkenes

The first efficient and well-characterized metal catalyst for the hydrogenation of alkenes was the Wilkinson catalyst.[122] This system was subsequently modified by Büthe,[123] Burk,[124] Kagan,[125] Knowles[126] and Noyori[127] through the introduction of chiral phosphines, which make the reaction enantioselective. The most important examples of this synthetic methodology were the asymmetric hydrogenation of dehydroamino acids by Knowles,[27] later applied to the industrial production of L-DOPA,[128] and the enantioselective hydrogenation processes developed by Noyori,[29] both of whom were awarded the Nobel Prize in chemistry in 2001.

Two different reaction mechanisms have been proposed for the catalytic asymmetric hydrogenation of alkenes, namely the hydride mechanism and the alkene mechanism. In the former, the first step is the oxidative addition of hydrogen to the catalyst, giving rise to a dihydride complex, which is followed by the coordination of the alkene to the metal. In the alkene pathway, the order in which these steps take place is reversed, *i.e.* the alkene coordination is followed by the formation of the dihydride. In both mechanisms, once the dihydride is formed and the alkene is bound to the metal, the reaction product is formed through a migratory insertion and a final reductive elimination.

The asymmetric hydrogenation of α-formamidoacrylonitrile catalyzed by $[Rh((R,R)\text{-Me-DuPHOS})]^+$ (see Fig. 13) was theoretically investigated by the group of Landis. The reaction mechanism was initially explored by means of a QM study on a model system,[51] in which DuPHOS was modelled as $(PH_3)_2$, using the DFT(B3LYP) method.[90,91] The origin of the enantioselectivity was subsequently determined through a QM/MM study on the real system[52] using the ONIOM method (ONIOM stands for "Our own N-layered Integrated molecular Orbital and molecular Mechanics").[129]

The preliminary mechanistic study[51] revealed that the reaction follows the alkene pathway. Four different *cis*-dihydride isomers can be formed in the oxidative addition, depending on the relative orientation of H_2 with respect to the alkene complex (see Fig. 14). The results showed that the **A** approach corresponds to the lowest energy pathway. The mechanism, characterized by Landis *et al.*, begins with the coordination of α-formamidoacrylonitrile to $[Rh((R,R)\text{-Me-DuPHOS})]^+$, followed by the formation of a van der Waals complex with hydrogen. The subsequent oxidative addition of H_2 leads to an

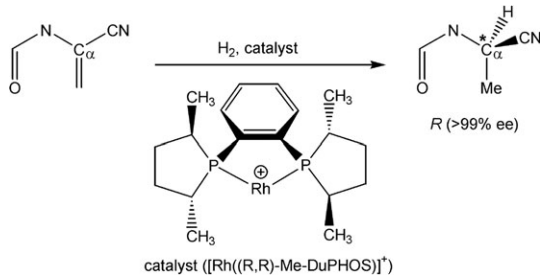

Fig. 13 Asymmetric hydrogenation of α-formamidoacrylonitrile catalyzed by $[Rh((R,R)\text{-Me-DuPHOS})]^+$.

octahedral rhodium complex, which undergoes two consecutive migratory insertions. In the last step, which is rate-determining, the final reaction product is obtained through reductive elimination. This mechanism disagrees with the commonly accepted one, in which the rate-determining step is the oxidative addition of hydrogen. Furthermore, this theoretical study revealed that the migratory insertion was irreversible and enantiodetermining, which was later supported by experimental studies.[130]

The ONIOM study[52] showed that the real system also follows the **A** pathway. The main difference, with respect to the model system, was found in the insertion barriers, which are significantly lower compared to those of the oxidative addition. The calculations indicated that the stereochemical outcome of the reaction was controlled by the anti-lock-and-key mechanism, as previously suggested by Burk *et al.*[131] In this mechanistic scheme, originally proposed by Halpern[132] and Brown,[133] there are two diastereomers of the alkene complex in equilibrium, and, whereas the major reaction product comes from the less stable intermediate, the minor reaction product is connected to the most abundant

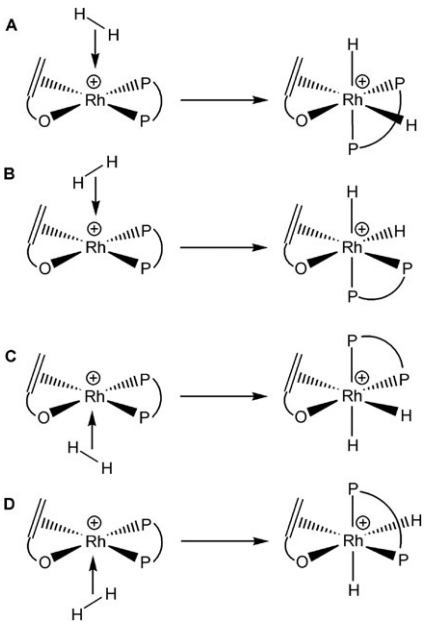

Fig. 14 Possible reaction pathways in the oxidative addition of H_2 to $[Rh((R,R)\text{-Me-DuPHOS})]^+$.

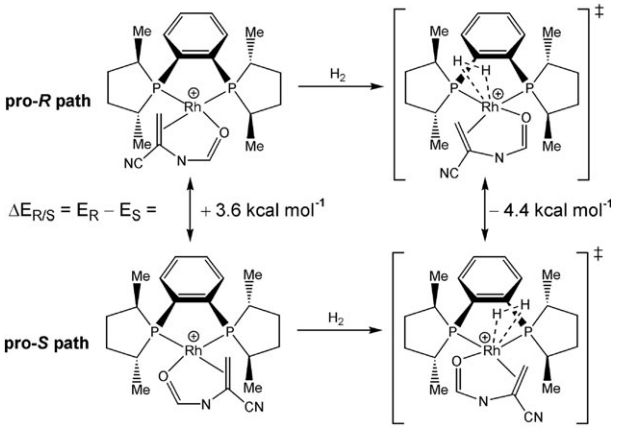

Fig. 15 Diastereomeric forms of the pro-*R* and pro-*S* alkene complexes (left) and transition states (right) in the asymmetric hydrogenation of α-formamidoacrylonitrile catalyzed by [Rh((*R*,*R*)-Me-DuPHOS)]$^+$.

intermediate. The QM/MM calculations predicted that the major product was the *R*-enantiomer, in total agreement with the experimental data. The results pointed out that the pro-*S* alkene complex was more stable than the pro-*R* complex by 3.6 kcal mol^{-1} (see Fig. 15). Nevertheless, the pro-*R* pathway was clearly favored over the pro-*S* at a kinetic level by an energy difference of 4.4 kcal mol^{-1}. This energy gap corresponds to a theoretical ee of 99.9%, within the range of experimental enantioselectivities obtained with [Rh((*R*,*R*)-Me-DuPHOS)]$^+$.[134]

A study on the real system was extended by Landis and Feldgus in order to rationalize the effect of the enamide R_α-substituent on the enantioselectivity.[135] The replacement of nitrile in this position by a *tert*-butyl group implied a reversal of enantioselectivity.[136] The calculations revealed that this modification of the substrate implied a change in the preferred reaction pathway, which became **C** instead of **A** (see Fig. 14). Since the **C**-pathway is pro-*S*, in contrast with **A**, which is pro-*R*, the authors predicted that with R_α = *tert*-butyl, the reaction was pro-*S* with $\Delta E_{R/S}$ = 6.5 kcal mol^{-1} (>99% ee), in total agreement with the experimental results.[136] Furthermore, the replacement of nitrile by a *tert*-butyl group reduces the energy gap between the pro-*R* and pro-*S* alkene complexes to almost zero (0.1 kcal mol^{-1}), and changes the order in which the two consecutive migratory insertions take place.

3.4 Vanadium-catalyzed synthesis of chiral sulfoxides

Certain chiral sulfoxides are of high interest due to their biological activity, such as the anti-ulcer agent esomeprazole.[137,138] The interest in chiral sulfoxides is also due to their two main properties: (1) high optical stabilities and (2) strongly asymmetric environments. Due to these properties, chiral sulfoxides have been widely applied in asymmetric synthesis,[139] both as chiral auxiliaries and chiral ligands. This interest in chiral sulfoxides has prompted the development of efficient synthetic methods to afford these compounds.[140] One of these methods, vanadium-catalyzed sulfoxidation with hydrogen peroxide[141–145] has been theoretically studied by ourselves.

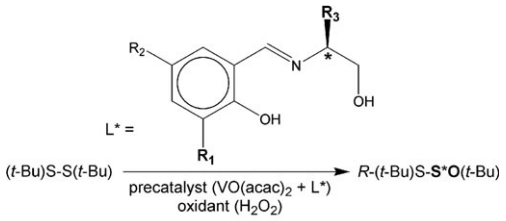

R1	R2	R3	Enantioselectivity
***t*-Bu**	*t*-Bu	***t*-Bu**	**82% ee**
t-Bu	H	*t*-Bu	83% ee
t-Bu	*t*-Bu	***i*-Pr**	**60% ee**
H	H	*t*-Bu	**46% ee**

Fig. 16 Vanadium-catalyzed asymmetric sulfoxidation of 1,2-bis (*tert*-butyl) disulfide with hydrogen peroxide.

In the sulfoxidation approach, optically active sulfoxides are obtained through the oxidation of a prochiral sulfide using vanadium complexes as catalysts and hydrogen peroxide as an oxidant. One of the most interesting examples of this synthetic method is the asymmetric oxidation of 1,2-bis(*tert*-butyl) disulfide reported by Ellman *et al.*[142] (see Fig. 16). The nature of the catalyst and the reaction mechanism of this catalytic system were essentially unknown. Mechanistic studies on reaction mixtures[146–148] pointed to a neutral oxo complex of vanadium(v) as the catalyst, characterized by a metal : ligand : peroxide ratio of 1 : 1 : 1. Nevertheless, such studies did not clarify whether hydrogen peroxide was bound to the metal as a hydroperoxo (HOO) or a peroxo (OO) ligand. Furthermore, the reaction mechanism was unknown, although the same mechanisms operating in the similar metal-catalyzed epoxidation reaction, namely the insertion and the direct oxygen transfer mechanisms,[149] were proposed.

These questions were tackled by our group in a QM study on a model system[56] using the DFT(B3LYP) method.[90,91] The results showed that: (1) the hydroperoxo complex was both the most stable and most active isomer of the catalyst, and (2) the reaction followed a direct oxygen transfer mechanism (see Fig. 17). Our calculations showed that the hydroperoxo form was

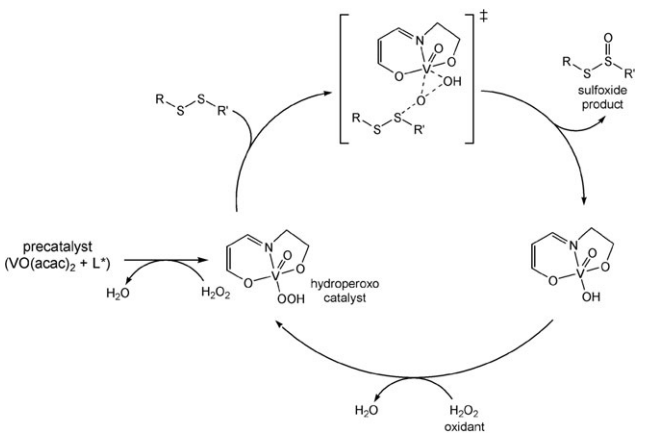

Fig. 17 Direct oxygen transfer mechanism with the hydroperoxo catalyst.

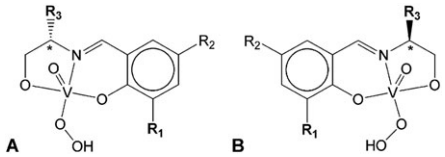

Fig. 18 **A** and **B** diastereomers of the vanadium catalyst for sulfoxidation.

more stable than the peroxo isomer by 4.4 kcal mol^{-1}. Moreover, the hydroperoxo complex catalyzed the sulfoxidation process, reducing its barrier from 40.4 to 26.7 kcal mol^{-1}.

Once the nature of the catalyst and the reaction mechanism were established, the origin of the enantioselectivity was explored by considering the real system in a QM/MM study[57] using the IMOMM method.[119] One of the most interesting features of the catalytic system represented in Fig. 16 is the strong influence of both R1 and R3 substituents on the enantioselectivity. This effect is quite puzzling, since these substituents are far from each other in the chiral ligand.

The vanadium atom of the hydroperoxo catalyst characterized in the study of this model system is stereogenic and because of its presence this species exists in two enantiomeric forms. These enantiomers become diastereomers (**A** and **B**, see Fig. 18) in the real system due to the presence of the chiral Schiff base ligand, which has a fixed configuration. The structures of **A** and **B**, and their associated sulfoxidation transition states, were optimized. We found that isomer **A** was more stable than **B** by 1.9 kcal mol^{-1}. The main structural difference between the species is given by the relative position of substituent R3, which occupies the oxo face of the catalyst in **B** and the opposite side in **A**. Interestingly, we found that both **A** and **B** catalyzed the oxidation of bis(*tert*-butyl) disulfide, but induced opposite enantioselectivities; whereas **A** was pro-*R*, **B** was pro-*S*. Our results pointed out that the major reaction product was *R*, in total agreement with the experimental results.[142] The most stable pro-*R* transition state was connected to diastereomer **A**. In contrast, the most stable pro-*S* saddle point was connected to **B**, and the participation of this isomer was thus crucial.

On the basis of our QM/MM calculations, we constructed a steric model, represented in Fig. 19, in order to rationalize the origin of the enantioselectivity. This model was able to explain the strong dependence of the enantioselectivity on the nature of both R1 and R3. For each isolated isomer, enantioselectivity was controlled by the energy gap between the pro-*R* and pro-*S* transition states: ΔE_A for **A** and ΔE_B for **B**. Both ΔE_A and ΔE_B were modulated by substituent R1, which discriminated the pro-*R* and pro-*S* pathways by introducing repulsive steric interactions with the *tert*-butyl group of the substrate. The steric bulk reduction resulting from the replacement of R1 = *t*-Bu with R1 = H implied a reduction of ΔE_A from 2.4 kcal mol^{-1} (90% ee) to 0.3 kcal mol^{-1} (21% ee), in good agreement with the experimental data[142] (see Fig. 16). Furthermore, enantioselectivity also depended on the energy gap between the most stable pro-*R* transition state, connected to **A**, and the most stable pro-*S* transition state, connected to **B**. This energy gap, labelled ΔE_{AB}, was influenced by R3, which provided the main structural difference between the **A** and **B**

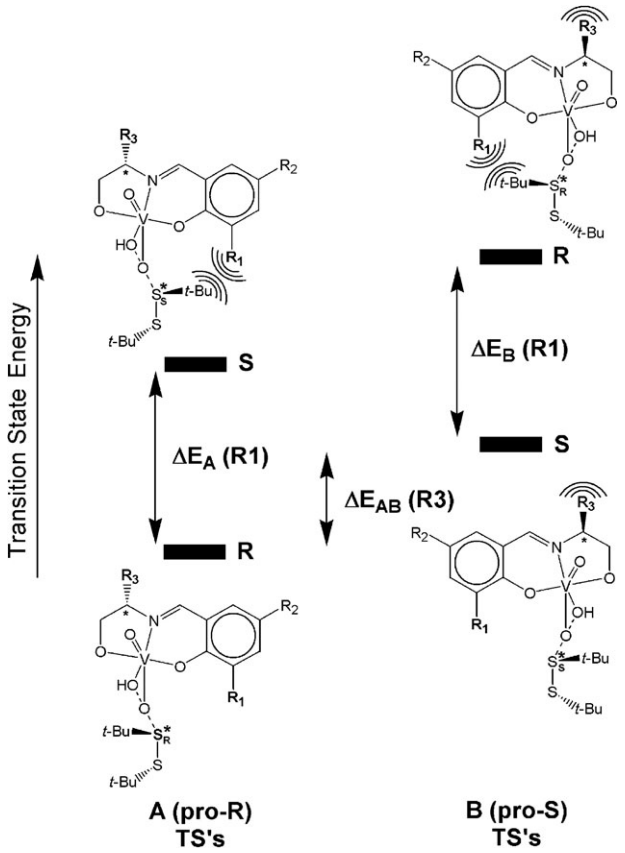

Fig. 19 Steric model for vanadium-catalyzed asymmetric sulfoxidation.

diastereomers of the catalyst. The steric bulk reduction offered by the replacement of R3 = *t*-Bu with R3 = *i*-Pr implied a reduction of ΔE_{AB} from 1.8 kcal mol^{-1} (90% ee) to 1.1 kcal mol^{-1} (74% ee), in good agreement with the experimental results.[142]

Our steric model allows the optimization of this catalytic system to be tackled by following a rational strategy. Enantioselectivity would rise, increasing the steric hindrance induced by the catalyst, firstly in the R3 position, in order to reduce the participation of the pro-*S* B form, and then in the R1 position, to amplify the pro-*R* character of the **A** diastereomer.

4. Conclusions and perspectives

The theoretical studies reviewed in this Perspective article demonstrate that computational chemistry can be used to obtain valuable insight into asymmetric synthesis. These studies give mechanistic pictures on a variety of reaction systems, and furthermore provided simple and useful steric models to rationalize the origin of enantioselectivity. These models can be used to test new chiral systems *in silico* and tackle their design in a rational fashion. The computational tools have changed over the years, but the more recent work has followed the pioneering tracks of Nguyen Trong Anh and Eisenstein 30 years ago.[1]

The ongoing development of new and more complex methods of asymmetric synthesis nowadays prompts the

community of theoretical chemists to improve the computational tools available. The time cost of QM calculations should be reduced, and the accuracy and range of applications of MM force fields should be extended. The treatment of reaction systems characterized by a large conformational space also needs to be improved. Furthermore, the development, application and refinement of steric models should be further stimulated through collaboration with experimental chemists.

Acknowledgements

Financial support from the ICIQ foundation, the Spanish MEC (projects CTQ2005-09000-CO1-02, Consolider Ingenio 2010 no. CSD2006-0003) and the Catalan DURSI (project 2005SGR00715) is acknowledged.

References

1 Nguyen Trong Anh and O. Eisenstein, *Nouv. J. Chim.*, 1977, **1**, 61.
2 E. W. Horton, *Chem. Soc. Rev.*, 1975, **4**, 589.
3 R. I. Christopherson, S. D. Lyons and P. K. Wilson, *Acc. Chem. Res.*, 2002, **35**, 961.
4 I. Gallou and C. H. Senanayake, *Chem. Rev.*, 2006, **106**, 2843.
5 A. R. Butler and Y.-L. Wu, *Chem. Soc. Rev.*, 1992, **21**, 85.
6 M. M. Green, K.-S. Cheon, S.-Y. Yang, J.-W. Park, S. Swansburg and W. Liu, *Acc. Chem. Res.*, 2001, **34**, 672.
7 G. Koeckelberghs, L. De Cremer, W. Vanormelingen, T. Verbiest, A. Persoons and C. Samyn, *Macromolecules*, 2005, **38**, 4545.
8 G. Zech and H. Kunz, *Chem.–Eur. J.*, 2004, **10**, 4136.
9 R. G. Xiong, J. L. Zuo, X. Z. You, B. F. Abrahams, Z. P. Bai, C. M. Che and H. K. Fun, *Chem. Commun.*, 2000, 2061.
10 M. R. Kurpiewski, M. Koziolkiewicz, A. Wilk, W. J. Stec and L. Jen-Jacobson, *Biochemistry*, 1995, **35**, 8846.
11 R. Peri, S. Padmanabhan, A. Rutledge, S. Singh and D. J. Triggle, *J. Med. Chem.*, 2000, **43**, 2906.
12 C. V. Kumar, A. Buranaprapuk and H. C. Sze, *Chem. Commun.*, 2001, 297.
13 H. Nakagawa, Y. Kobori, M. Yoshida and K. Yamada, *Chem. Commun.*, 2001, 2692.
14 J. J. L. M. Cornelissen, A. E. Rowan, R. J. M. Nolte and N. A. J. M. Sommerdijk, *Chem. Rev.*, 2001, **101**, 4039.
15 M. Harmata, *Acc. Chem. Res.*, 2004, **37**, 862.
16 V. A. Mallia and N. Tamaoki, *Chem. Soc. Rev.*, 2000, **33**, 76.
17 C. Ruslim and K. Ichimura, *J. Mater. Chem.*, 2002, **12**, 3377.
18 S. C. Stinson, *Chem. Eng. News*, 2001, **79**, 77.
19 G. W. Mellin and M. Katzenstein, *N. Engl. J. Med.*, 1962, **267**, 1184.
20 J. Tomaszewski and M. M. Rumore, *Drug Dev. Ind. Pharm.*, 1994, **20**, 119.
21 A. M. Thayer, *Chem. Eng. News*, 2006, **84**, 29.
22 S. Hata, M. Iguchi, T. Iwasawa, K.-i. Yamada and K. Tomioka, *Org. Lett.*, 2004, **6**, 1721.
23 M. N. Masuno, D. M. Young, A. C. Hoepker, C. K. Skepper and T. F. Molinski, *J. Org. Chem.*, 2005, **70**, 4162.
24 F. A. Davis and B. C. Chen, *Chem. Rev.*, 1992, **95**, 919.
25 W. Adam, M. N. Korb, K. J. Roschmann and C. R. Saha-Moller, *J. Org. Chem.*, 1998, **63**, 3423.
26 E. N. Jacobsen, A. Pfaltz and H. Yamamoto, *Comprehensive Asymmetric Catalysis*, Springer, Berlin, 1999.
27 W. S. Knowles, *Angew. Chem., Int. Ed.*, 2002, **41**, 1998.
28 K. B. Sharpless, *Angew. Chem., Int. Ed.*, 2002, **41**, 2024.
29 R. Noyori, *Angew. Chem., Int. Ed.*, 2002, **41**, 2008.
30 R. E. Gawley, *J. Org. Chem.*, 2006, **71**, 2411.
31 A. R. Leach, *Molecular Modelling*, Prentice Hall, Harlow, 2001.
32 I. N. Levine, *Quantum Chemistry*, Prentice Hall, Harlow, 1999.
33 W. Koch and M. C. Holthausen, *A Chemist's Guide to Density Functional Theory*, Wiley-VCH, Weinheim, 2001.
34 M. Torrent, M. Sola and G. Frenking, *Chem. Rev.*, 2000, **100**, 439.
35 T. Ziegler and J. Autschbach, *Chem. Rev.*, 2005, **105**, 2695.
36 D. G. Musaev and K. Morokuma, in *Theoretical Aspects of Transition Metal Catalysis*, ed. G. Frenking, Springer, Berlin, 2005, pp. 1.
37 S. Sakaki and Y. Musashi, in *Computational Modeling of Homogeneous Catalysis*, ed. F. Maseras and A. Lledós, Kluwer, Dordrecht, 2002, pp. 79.
38 A. Michalak and T. Ziegler, in *Theoretical Aspects of Transition Metal Catalysis*, ed. G. Frenking, Springer, Berlin, 2005, pp. 145.
39 E. Clot and O. Eisenstein, in *Computational Modeling of Homogeneous Catalysis*, ed. F. Maseras and A. Lledós, Kluwer, Dordrecht, 2002, pp. 137.
40 D. V. Deubel, C. Loschen and G. Frenking, in *Theoretical Aspects of Transition Metal Catalysis*, ed. G. Frenking, Springer, Berlin, 2005, pp. 109.
41 M. Solà, M. Duran and M. Torrent, in *Computational Modeling of Homogeneous Catalysis*, ed. F. Maseras and A. Lledós, Kluwer, Dordrecht, 2002, pp. 269.
42 A. Sundermann, O. Uzan and J. M. L. Martin, *Chem.–Eur. J.*, 2001, **7**, 1703.
43 A. A. C. Braga, N. H. Morgon, G. Ujaque and F. Maseras, *J. Am. Chem. Soc.*, 2005, **127**, 9298.
44 R. Álvarez, O. N. Faza, C. S. López and A. R. de Lera, *Org. Lett.*, 2006, **8**, 35.
45 R. J. Deeth and N. Fey, *Organometallics*, 2004, **23**, 1042.
46 K. B. Lipkowitz, C. A. D'Hue, T. Sakamoto and J. N. Stack, *J. Am. Chem. Soc.*, 2002, **124**, 14255.
47 P.-O. Norrby, T. Rasmussen, J. Haller, T. Strassner and K. N. Houk, *J. Am. Chem. Soc.*, 1999, **121**, 10186.
48 F. Jensen and P.-O. Norrby, *Theor. Chim. Acta*, 2003, **109**, 1.
49 F. Maseras, *Chem. Commun.*, 2000, 1821.
50 G. Ujaque and F. Maseras, *Struct. Bonding*, 2004, **112**, 117.
51 C. R. Landis, P. Hilfenhaus and S. Feldgus, *J. Am. Chem. Soc.*, 1999, **121**, 8741.
52 S. Feldgus and C. R. Landis, *J. Am. Chem. Soc.*, 2000, **122**, 12714.
53 T. Matsubara, N. Koga, Y. Ding, D. G. Musaev and K. Morokuma, *Organometallics*, 1997, **16**, 1065.
54 J. J. Carbo, F. Maseras, C. Bo and P. W. N. M. van Leeuwen, *J. Am. Chem. Soc.*, 2001, **123**, 7630.
55 A. Magistrato, T. K. Woo, A. Togni and U. Rothlisberger, *Organometallics*, 2004, **23**, 3218.
56 D. Balcells, F. Maseras and A. Lledós, *J. Org. Chem.*, 2003, **68**, 4265.
57 D. Balcells, F. Maseras and G. Ujaque, *J. Am. Chem. Soc.*, 2005, **127**, 3624.
58 S. Dapprich, G. Ujaque, F. Maseras, A. Lledós, D. G. Musaev and K. Morokuma, *J. Am. Chem. Soc.*, 1996, **118**, 11660.
59 G. Ujaque, F. Maseras and A. Lledós, *J. Am. Chem. Soc.*, 1999, **121**, 1317.
60 T. K. Woo, L. Fan and T. Ziegler, *Organometallics*, 1994, **13**, 2252.
61 D. G. Musaev, R. D. J. Froese and K. Morokuma, *Organometallics*, 1998, **17**, 1850.
62 G. Guerra, L. Cavallo, G. Moscardi, M. Vacatello and P. Corradini, *J. Am. Chem. Soc.*, 1994, **116**, 2988.
63 L. Resconi, L. Cavallo, A. Fait and F. Piemontesi, *Chem. Rev.*, 2000, **100**, 1253.
64 D. A. Evans, C. S. Burgey, M. C. Kozlowski and S. W. Tregay, *J. Am. Chem. Soc.*, 1999, **121**, 686.
65 T. Rasmussen and P.-O. Norrby, *J. Am. Chem. Soc.*, 2003, **125**, 5130.
66 M. C. Kozlowski, S. L. Dixon, M. Panda and G. Lauri, *J. Am. Chem. Soc.*, 2003, **125**, 6614.
67 D. A. Evans, S. J. Siska and V. J. Cee, *Angew. Chem., Int. Ed.*, 2003, **42**, 1761.
68 V. J. Cee, C. J. Cramer and D. A. Evans, *J. Am. Chem. Soc.*, 2006, **128**, 2920.
69 D. J. Cram and F. A. A. Elhafez, *J. Am. Chem. Soc.*, 1952, **74**, 5828.
70 J. W. Cornforth, R. H. Cornforth and K. K. Mathew, *J. Chem. Soc.*, 1959, 112.
71 G. J. Karabatsos, *J. Am. Chem. Soc.*, 1967, **89**, 1367.
72 M. Chérest, H. Felkin and N. Prudent, *Tetrahedron Lett.*, 1968, 2201.
73 M. Chérest and H. Felkin, *Tetrahedron Lett.*, 1968, 2205.

74 K. N. Houk, *Theor. Chem. Acc.*, 2000, **103**, 330.
75 G. C. Fu, *Acc. Chem. Res.*, 2004, **37**, 542.
76 B. List, *Acc. Chem. Res.*, 2004, **37**, 548.
77 W. Notz, F. Tanaka and C. F. Barbas III, *Acc. Chem. Res.*, 2004, **37**, 580.
78 S. J. Miller, *Acc. Chem. Res.*, 2004, **37**, 601.
79 A. Thayer, *Chem. Eng. News*, 2005, **83**, 55.
80 Z. G. Hajos and D. R. Parrish, *J. Org. Chem.*, 1974, **39**, 1615.
81 U. Eder, G. Sauer and R. Wiechert, *Angew. Chem., Int. Ed. Engl.*, 1971, **10**, 496.
82 N. Cohen, *Acc. Chem. Res.*, 1976, **9**, 412.
83 A. B. Smith III, J. Kingery-Wood, T. L. Leenay, E. G. Nolen and T. Sunazuka, *J. Am. Chem. Soc.*, 1992, **114**, 1438.
84 T. Nagamitsu, T. Sunazuka, R. Obata, H. Tomoda, H. Tanaka, Y. Harigaya, S. Omura and A. B. Smith III, *J. Org. Chem.*, 1995, **60**, 8126.
85 S. J. Danishefsky, J. J. Masters, W. B. Young, J. T. Link, L. B. Snyder, T. V. Magee, D. K. Jung, R. C. A. Isaacs, W. G. Bornmann, C. A. Alaimo, C. A. Coburn and M. J. DiGrandi, *J. Am. Chem. Soc.*, 1996, **118**, 2843.
86 T. A. Spencer, H. S. Neel, T. W. Flechtner and R. A. Zayle, *Tetrahedron Lett.*, 1965, **6**, 3889.
87 H. Molines and C. Wakselman, *Tetrahedron*, 1976, **32**, 2099.
88 K. L. Brown, L. Damm, J. D. Dunitz and A. Eschenmoser, *Helv. Chim. Acta*, 1978, **61**, 3108.
89 C. Allemann, R. Gordillo, F. R. Clemente, P. H.-Y. Cheong and K. N. Houk, *Acc. Chem. Res.*, 2004, **37**, 558.
90 A. D. Becke, *J. Chem. Phys.*, 1993, **98**, 5648.
91 C. Lee, R. G. Parr and W. Yang, *Phys. Rev. B: Condens. Matter*, 1988, **37**, 785.
92 F. R. Clemente and K. N. Houk, *Angew. Chem., Int. Ed.*, 2004, **43**, 5766.
93 F. R. Clemente and K. N. Houk, *J. Am. Chem. Soc.*, 2005, **127**, 11294.
94 L. Hoang, S. Bahmanyar, K. N. Houk and B. List, *J. Am. Chem. Soc.*, 2003, **125**, 16.
95 S. Bahmanyar and K. N. Houk, *J. Am. Chem. Soc.*, 2001, **123**, 12911.
96 S. Bahmanyar, K. N. Houk, H. J. Martin and B. List, *J. Am. Chem. Soc.*, 2003, **125**, 2475.
97 S. Bahmanyar and K. N. Houk, *Org. Lett.*, 2003, **5**, 1240.
98 P. H.-Y. Cheong and K. N. Houk, *J. Am. Chem. Soc.*, 2004, **126**, 13912.
99 R. Gordillo, J. Carter and K. N. Houk, *Adv. Synth. Catal.*, 2004, **346**, 1175.
100 R. Gordillo and K. N. Houk, *J. Am. Chem. Soc.*, 2006, **128**, 3543.
101 W. D. Cornell, P. Cieplak, C. I. Bayly, I. R. Gould, K. M. Merz, D. M. Ferguson, D. C. Spellmeyer, T. Fox, J. W. Caldwell and P. A. Kollman, *J. Am. Chem. Soc.*, 1995, **117**, 5179.
102 D. Craig, *Chem. Soc. Rev.*, 1987, **16**, 187.
103 U. Pindur, G. Lutz and C. Otto, *Chem. Rev.*, 1993, **93**, 741.
104 D. Carmona, M. P. Lamata and L. A. Oro, *Coord. Chem. Rev.*, 2000, **200**, 717.
105 E. J. Corey, *Angew. Chem., Int. Ed.*, 2002, **41**, 1650.
106 K. B. Lipkowitz and M. C. Kozlowski, *Synlett*, 2003, 1547.
107 K. B. Lipkowitz, T. Sakamoto and J. Stack, *Chirality*, 2003, **15**, 759.
108 K. Narasaka, N. Iwasawa, M. Inoue, T. Yamada, M. Nakashima and J. Sugimori, *J. Am. Chem. Soc.*, 1989, **111**, 5340.
109 H. C. Kolb, M. S. VanNieuwenhze and K. B. Sharpless, *Chem. Rev.*, 1994, **94**, 2483.
110 E. N. Jacobsen, I. Marko, W. S. Mungall, G. Schroeder and K. B. Sharpless, *J. Am. Chem. Soc.*, 1988, **110**, 1968.
111 K. B. Sharpless, W. Amberg, Y. K. Bennani, G. A. Crispino, J. Hartung, K.-S. Jeong, K. Kwong, H.-L. Morikawa, D. Wang, Z.-M. Xu and X.-L. Zhang, *J. Org. Chem.*, 1992, **57**, 2768.
112 K. B. Sharpless, A. Y. Teranishi and J.-E. Backvall, *J. Am. Chem. Soc.*, 1977, **99**, 3120.
113 T. Gobel and K. B. Sharpless, *Angew. Chem., Int. Ed. Engl.*, 1993, **32**, 1329.
114 P.-O. Norrby, H. C. Kolb and K. B. Sharpless, *Organometallics*, 1994, **13**, 344.
115 E. J. Corey, P. D. Jardine, S. Virgil, P.-W. Yuen and R. D. Connell, *J. Am. Chem. Soc.*, 1989, **111**, 9243.
116 E. J. Corey, M. C. Noe and S. Sarshar, *J. Am. Chem. Soc.*, 1993, **115**, 3828.
117 D. V. Deubel and G. Frenking, *Acc. Chem. Res.*, 2003, **36**, 645.
118 G. Drudis-Sole, G. Ujaque, F. Maseras and A. Lledos, *Chem.–Eur. J.*, 2005, **11**, 1017.
119 F. Maseras and K. Morokuma, *J. Comput. Chem.*, 1995, **16**, 1170.
120 E. J. Corey and M. C. Noe, *J. Am. Chem. Soc.*, 1996, **118**, 11038.
121 H. Becker, S. B. King, M. Taniguchi, K. P. M. Vanhessche and K. B. Sharpless, *J. Org. Chem.*, 1995, **60**, 3940.
122 J. A. Osborn, F. H. Jardine, J. F. Young and G. Wilkinson, *J. Chem. Soc. A*, 1966, 1711.
123 L. Horner, H. Siegel and H. Büthe, *Angew. Chem., Int. Ed. Engl.*, 1968, **7**, 942.
124 M. J. Burk, *J. Am. Chem. Soc.*, 1991, **113**, 8518.
125 T. P. Dang and H. B. Kagan, *J. Am. Chem. Soc.*, 1972, **94**, 6429.
126 W. S. Knowles and M. J. Sabacky, *Chem. Commun. (London)*, 1968, 1445.
127 A. Miyashita, A. Yasuda, H. Takaya, K. Toriumi, T. Ito, T. Souchi and R. Noyori, *J. Am. Chem. Soc.*, 1980, **102**, 7932.
128 W. S. Knowles, *J. Chem. Educ.*, 1986, **63**, 222.
129 S. Dapprich, I. Komaromi, K. S. Byun, K. Morokuma and M. Frisch, *J. Mol. Struct. (THEOCHEM)*, 1999, **461–462**, 1.
130 I. D. Gridnev, N. Higashi, K. Asakura and T. Imamoto, *Adv. Synth. Catal.*, 2001, **343**, 118.
131 S. K. Armstrong, J. M. Brown and M. J. Burk, *Tetrahedron Lett.*, 1993, **34**, 879.
132 A. S. C. Chan and J. Halpern, *J. Am. Chem. Soc.*, 1980, **102**, 838.
133 J. M. Brown and D. Parker, *Organometallics*, 1982, **1**, 950.
134 M. J. Burk, J. E. Feaster, W. A. Nugent and R. L. Harlow, *J. Am. Chem. Soc.*, 1993, **115**, 10125.
135 S. Feldgus and C. R. Landis, *Organometallics*, 2001, **20**, 2374.
136 M. J. Burk, G. Casy and N. B. Johnson, *J. Org. Chem.*, 1998, **63**, 6084.
137 H. Cotton, T. Elebring, M. Larsson, L. Li, H. Sörensen and S. von Unge, *Tetrahedron: Asymmetry*, 2000, **11**, 3819.
138 J. Renfrey and S. Featherstone, *Nat. Rev. Drug Discovery*, 2002, **1**, 175.
139 M. C. Carreño, *Chem. Rev.*, 1995, **95**, 1717.
140 I. Fernández and N. Khiar, *Chem. Rev.*, 2003, **103**, 3651.
141 C. Bolm and F. Binewald, *Angew. Chem., Int. Ed. Engl.*, 1995, **34**, 2640.
142 A. D. Cogan, G. Liu, K. Kim, B. J. Backes and J. A. Ellman, *J. Am. Chem. Soc.*, 1998, **120**, 8011.
143 A. H. Vetter and A. Berkessel, *Tetrahedron Lett.*, 1998, **39**, 1741.
144 J. Skarzewski, E. Wojazczynska and I. Turowska-Tyrk, *Tetrahedron: Asymmetry*, 2002, **13**, 369.
145 C. Drago, L. Caggiano and R. F. W. Jackson, *Angew. Chem., Int. Ed.*, 2005, **44**, 7221.
146 S. A. Blum, R. G. Bergman and J. A. Ellman, *J. Org. Chem.*, 2003, **68**, 150.
147 N. N. Karpyshev, O. D. Yakovleva, E. P. Talsi, K. P. Bryliakov, O. V. Tolstikova and A. G. Tolstikov, *J. Mol. Catal. A: Chem.*, 2000, **157**, 91.
148 K. P. Bryliakov, N. N. Karpyshev, S. A. Fominsky, A. G. Tolstikov and E. P. Talsi, *J. Mol. Catal. A: Chem.*, 2001, **171**, 73.
149 N. Rösch, C. Di Valentin and I. V. Yudanov, in *Computational Modeling of Homogeneous Catalysis*, ed. F. Maseras and A. Lledós, Kluwer, Dordrecht, 2002, pp. 289.